scientific reports

Check for updates

OPEN

Lymphocyte antigen 6 family member E suppresses apoptosis and promotes pancreatic cancer growth and migration via Wnt/β-catenin pathway activation

Kenan Cen[1,5], Jingyao Zhou[2,5], Xuejia Yang[3,5], Yangyang Guo[3] & Yanyi Xiao[4]✉

Pancreatic cancer (PC) is the primary cause of cancer-related mortality. Due to the absence of reliable biomarkers for predicting prognosis or guiding treatment, there is an urgent need for molecular studies on PC. Lymphocyte antigen 6 family member E (LY6E) is implicated in uncontrolled cell growth across various cancers. However, the precise mechanism of LY6E in PC remains unclear. Here, we conducted comprehensive bioinformatic analyses using online tools and R-×64–4.1.1, complemented by experimental validation through Western blotting, immunohistochemistry, immunosorbent assays, flow cytometry, cell assays, and animal models. Our findings reveal significantly elevated expression of LY6E in PC, correlating with poor prognosis. LY6E knockdown inhibited proliferation, invasion, and migration of PC cells, while enhancing apoptosis evidenced by increased cleaved caspase 3 levels and alterations in the Bcl-2/Bax ratio. Conversely, LY6E overexpression promoted PC cell proliferation and migration, and inhibited apoptosis. Mechanistically, LY6E downregulation suppressed the Wnt/β-catenin signaling pathway. In vivo studies demonstrated that LY6E suppression attenuated tumor growth in murine models. Additionally, LY6E suppression resulted in reduced tumor growth in mice. In conclusion, our study confirms the significant role of LY6E in the progression of PC. LY6E, serving as an independent prognostic indicator, has the potential to serve as a valuable biomarker for PC to inform treatment strategies.

Keywords Pancreatic cancer, LY6E, Prognosis, Apoptosis, Wnt/β-catenin

Pancreatic cancer (PC) is a highly malignant solid tumor of the digestive system with an unfavorable prognosis, been a leading cause of cancer-related deaths in recent decades[1]. The number of diagnosed cases worldwide has doubled from 196,000 in 1990 to 441,000 in 2017[2]. The rise in incidence can be attributed not only to increased life expectancy and unhealthy habits but also to more precise and comprehensive early detection methods[3–6]. However, due to in-depth research and better management of PC, the mortality rates associated with this disease are on the decline[7]. Accumulating evidence supported that cancer is a special disease closely related with abnormal genome; there is no exception to PC[8–10]. Actually, genomic studies of PC have been explored and some fascinating discoveries have been used to guide treatment, all of which led to our preliminary triumph over the PC. Despite these advancements, further exploration at the molecular level is urgently needed due to the high heterogeneity and aggressiveness of PC.

Research on a notable cell surface protein associated with cancer, lymphocyte antigen 6 family member E (LY6E), encoded by the LY6E gene on human chromosome 8, has garnered attention[11]. LY6E is a cell membrane protein associated with interferon-induced glycosylphosphatidylinositol (GPI) and is found to be significantly overexpressed in various solid tumors, including pancreatic cancer[12]. A recent study suggests that high expression

[1]The Dingli Clinical College of Wenzhou Medical University, Wenzhou, China 325000. [2]Department of Pharmacy, Taizhou Central Hospital, Taizhou, China. [3]Zhejiang Key Laboratory of Intelligent Cancer Biomarker Discovery and Translation, The First Affiliated Hospital, Wenzhou Medical University, Wenzhou 325035, China. [4]Department of Thyroid and Breast Surgery, The Second Affiliated Hospital of Shanghai University, Wenzhou 325000, Zhejiang Province, China. [5]These authors contributed equally: Kenan Cen, Jingyao Zhou and Xuejia Yang. ✉email: 15967411128@163.com

of LY6E in neutrophils predicts the responsiveness to immunotherapy in humans[13]. Immunotherapy is primarily used to treat a variety of cancers, particularly those that are difficult to treat malignancies. Tokhanbigli et al. demonstrated that LY6E is significantly overexpressed in various gastrointestinal (GI) carcinomas, such as colorectal, gastric, and pancreatic cancer (PC). They reported that the LY6E peptide can modulate immune responses to colon cancer in mice, and dendritic cells loaded with LY6E peptide can enhance T cell proliferation to combat tumor growth[14]. Additionally, Yeom et al. confirmed that the upregulation of LY6E results in increased expression of HIF-1α at the transcriptional level, subsequently leading to the upregulation of vascular endothelial growth factor A (VEGFA) and platelet-derived growth factor subunit B (PDGFB) through the activation of the phosphatidylinositol 3'-kinase (PI3K)/protein kinase B (Akt) pathway, thereby promoting tumor angiogenesis and progression[15]. Moreover, Gou et al. confirmed that overexpression of LY6E in the PC stem cells can be detected, which might partly explain the aggressive characteristic of this disease[16]. Nevertheless, the precise role of LY6E in pancreatic cancer remains unclear, prompting the need for further investigation.

The tumor microenvironment (TME) comprises various immune and stromal cells (including endothelial cells, fibroblasts, natural killer cells, T cells, macrophages, etc.) as well as the extracellular matrix[17]. Previous research has highlighted the significant impact of the TME on tumor progression, metastasis, and responses to immunotherapy through the diverse functions of cancer-associated cells within the TME[18,19]. As to the PC, abundant evidence showed that TME plays a vital role in its tumorigenesis and progression[20,21]. Furthermore, emerging evidence suggests that LY6E may influence immune responses, contributing to immune regulation during viral infections and potentially mediating immune evasion during tumor development[16,22]. However, the specific functions and mechanisms of LY6E within the TME in driving tumor progression remain poorly understood and warrant further investigation.

This study aims to elucidate the functional role of LY6E in pancreatic cancer development and to delineate the significance of the Wnt/β-catenin signaling pathway and apoptosis in mediating LY6E regulation. Thus, based on previous evidence and bioinformatic analysis, we hypothesized that LY6E is abnormally expressed in PC which promotes tumorous proliferation and migration through up-regulating Wnt/β-catenin signaling pathway and suppressing apoptosis. Besides, we proposed that LY6E may relate to TME and immunotherapy responses. Our study may provide a guide for PC therapy.

Results

Expression profile of LY6E and its relationship with clinical characteristics across TCGA and GEO datasets

The mRNA expression profile demonstrated significantly enhanced LY6E expression in PC samples compared to normal tissues across datasets including "TCGA + GTEx," "GSE16515," "GSE32676," "GSE15471," and "GSE55463" ($P < 0.05$) (Fig. 1A). Moreover, PC samples with higher T stages and tumor grades exhibited elevated LY6E expression levels ($P < 0.05$) (Fig. 1B). Furthermore, PC cases with low and high LY6E expression levels showed significant differences in race, clinical stage, and tumor grade ($P < 0.05$) (Fig. 1C). Moreover, the Sanky plot showed the correlation between LY6E expression and clinical characteristics (Fig. 1D).

Prognostic ability of LY6E and construction of a nomogram

Patients with PC were stratified into low-expression and high-expression groups based on the median LY6E expression level. Notably, individuals exhibiting high LY6E expression showed decreased survival duration and increased mortality rates compared to those with low LY6E expression (Fig. 2A). Based on the TCGA-PAAD dataset, the high-expression group of PC exhibited significantly poorer prognosis compared to the low-expression group (hazard ratio [HR] = 1.829, 95% confidence interval [CI] = 1.208–2.768, $P = 0.00431$) (Fig. 2B). This trend was similarly observed in the GSE57495 and ICGC-PACA-AU datasets (Supplementary Fig. 1). The ROC analysis showed stable prognostic power of the LY6E expression (Fig. 2C). From the univariate and multivariate Cox regression analyses, LY6E expression and age were confirmed two independent prognostic factors (Fig. 2D). Sequentially, a nomogram was developed to predict the 1- and 3-year survival of each PC patient based on LY6E expression and age (Fig. 2E). The calibration curve demonstrated robust predictive accuracy of the nomogram (Fig. 2F).

Correlation analysis between LY6E expression and immunity

As is shown in Fig. 3A, a significant correlation was identified between LY6E expression and dendritic cells, B cells, macrophages, NK cells, CD4 + T cells, CD8 + T cells, and plasma cells ($P < 0.05$). To further verify the TME, we analyzed the immune cell infiltration in low-expression and high-expression PC, confirming that there is a significant difference in B cells, plasma cells, T cells, NK cells, and macrophages, consisting with the correlation analysis (Fig. 3B). Additionally, the relationship between each immune cell type and tumor mutation burden (TMB) and LY6E expression were presented in the Fig. 3C–K. Moreover, the association between LY6E and other immune-related genes was presented with a heatmap (Fig. 3L).

LY6E highly expresses in pancreatic cancer

To assess the expression of LY6E in PC, immunohistochemistry staining and Western blotting analysis for PC tissues and para-cancer tissue were performed, both of which demonstrated the higher expression of LY6E in the PC tissues than normal tissues (Fig. 4A, B). Sequentially, the expression of LY6E was detected in one pancreatic cell line and three PC cell lines using Western blotting, finding two pancreatic cell lines had significantly higher expression of LY6E including BxPC-3 and Patu8988 (Fig. 4C).

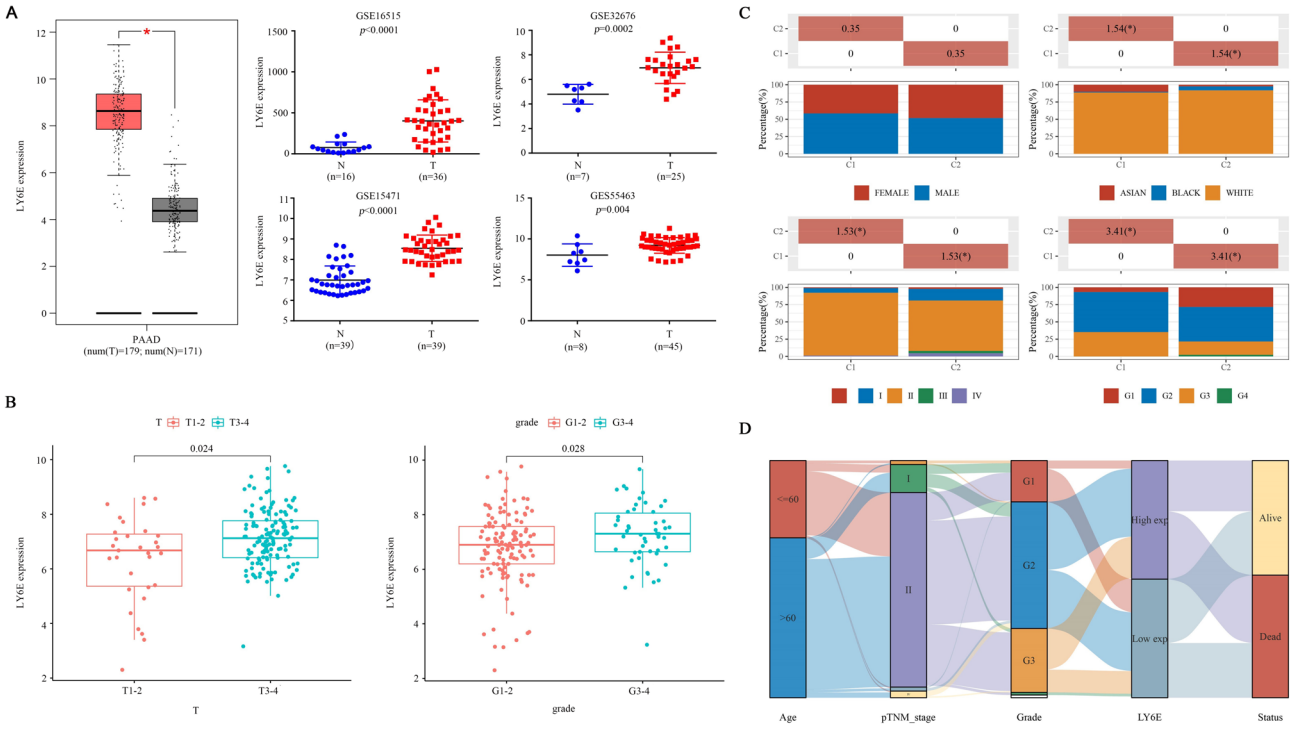

Fig. 1. LY6E expression and relationship with clinical characteristics in PC. (**A**) LY6E expression between PC tissues and normal tissues across TCGA + GTEx, GSE16515, GSE32676, GSE15471, and GSE55463 datasets. (**B**) LY6E expression difference in PC with different clinical subgroups. (**C**) Clinical characteristic difference in LY6E low-expression (C1) and high-expression (C2) subgroups. (**D**) Correlation between LY6E expression, age, clinical stage, tumor grade, and survival status. *, $p < 0.05$.

High expression of LY6E promotes pancreatic cancer cell proliferation in vitro

To evaluate the function of LY6E in PC, we conducted cell experiments. Lentivirus-based shRNA targeting LY6E was used to infect the BxPC-3 and Patu8988 PC cell lines, while the qRT-PCR and Western blotting analysis showed the efficient knockdown of LY6E with the shLY6E-1 and shLY6E-2 (Fig. 4D and E). CCK-8 assay analysis showed that after knockdown of LY6E, the proliferation of BxPC-3 and Patu8988 PC cells were significantly inhibited (Fig. 4F). Besides, fewer colonies of BxPC-3 and Patu8988 PC cells were formed after infecting with lenti-shLY6E-1 or lenti-shLY6E-2 (Fig. 4G). Immunofluorescence detected decrease of Ki67 in BxPC-3 and Patu8988 PC cells transfected with lenti-shLY6E-1 or lenti-shLY6E-2, which meat restraint of cancer cell growth after knockdown of LY6E (Fig. 4H).

Knockdown of LY6E promotes cleaved caspase-dependent apoptosis in pancreatic cancer

To explore the possible mechanisms of LY6E in regulating PC growth, we analyzed the apoptosis in BxPC-3 and Patu8988 cells transfected with lenti-shLY6E-1 or lenti-shLY6E-2. Flow cytometry showed that knockdown of LY6E significantly increased the apoptosis in BxPC-3 and Patu8988 PC cells (Fig. 5A). Then, the cleaved caspase 3, Bcl-2, and Bax proteins were detected by Western blotting, confirmed the increase of cleaved caspase 3 protein and Bax protein and decrease of Bcl-2 protein in BxPC-3 and Patu8988 PC cells after knockdown of LY6E (Fig. 5B). Immunofluorescence further demonstrated the higher expression of cleaved caspase 3 protein after knockdown of LY6E (Fig. 5C).

Knockdown of LY6E suppresses migration and invasion of pancreatic cancer

To investigate the effect of LY6E in migration of PC, we conducted in vitro experiments for analysis. Wound healing assays showed that knockdown of LY6E significantly inhibited the migration of BxPC-3 and Patu8988 PC cells (Fig. 6A). Additionally, invasion analysis revealed that the invasion ability of BxPC-3 and Patu8988 cells with lenti-shLY6E-1 or lenti-shLY6E-2 was significantly decreased (Fig. 6B). To explore the mechanism, Western blotting analysis showed that migration-related proteins including vimentin, E-Cadherin, and N-Cadherin were significantly affected by the knockdown of LY6E, which led to the suppression of migration and invasion in BxPC-3 and Patu8988 PC cells (Fig. 6C). Immunofluorescence confirmed the decrease of vimentin protein in BxPC-3 and Patu8988 cells after knockdown of LY6E (Fig. 6D).

LY6E overexpression enhances proliferation and migration of PC cells, while inhibiting apoptosis

LY6E overexpression was validated to elucidate its functional role in PANC-1 cells. The results showed that LY6E overexpression significantly enhanced cell viability at 24, 48, and 72 h (Fig. 7A) and promoted colony formation

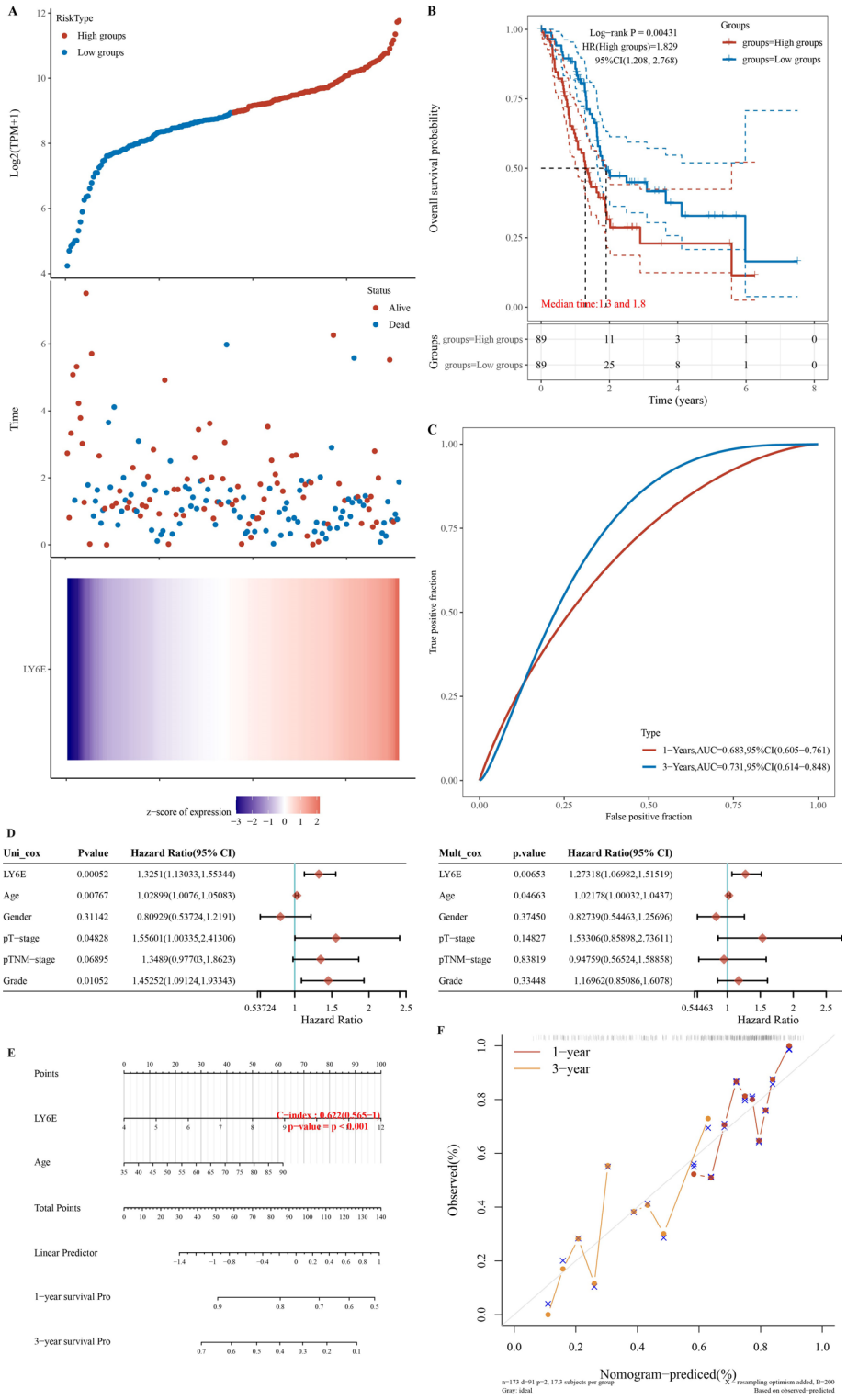

Fig. 2. Correlation of prognostic ability of LY6E expression. (**A**) Distribution, survival status plot, survival time of LY6E expression in TCGA-PAAD project. Red dots and blue dots represent patients with high and low expression of LY6E, respectively. (**B**) Survival analysis of LY6E low-expression and high-expression PC in TCGA-PAAD project. (**C**) ROC curves analyses between LY6E low-expression and high-expression PC in TCGA-PAAD project. (**D**) Univariate and multivariate Cox regression analyses in TCGA-PAAD project. (**E**) A nomogram of LY6E expression and age for PC. (**F**) A calibration plot for assessing the predictive ability of the nomogram at 1- and 3-year.

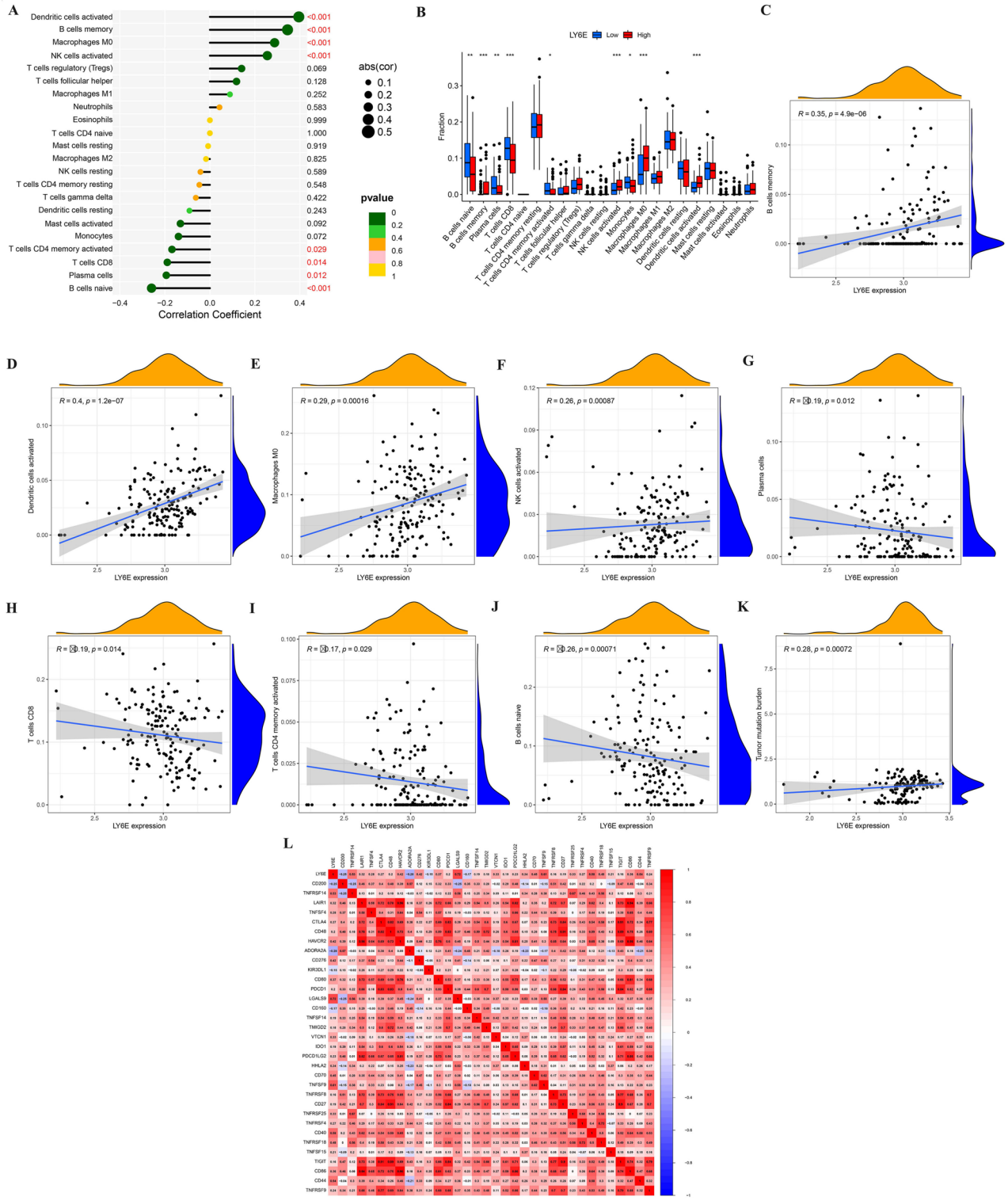

Fig. 3. Relationship of LY6E and immunity. (**A**) Correlation coefficient value between LY6E expression and immune cell infiltration. (**B**) Immune cell infiltration difference between LY6E low-expression and high-expression PC. (**C**, **D**, **E**, **F**, **G**, **H**, **I**, **J**, and **K**) Relationship between LY6E expression and memory B cells, activated dendritic cells, macrophage M0, activated NK cells, plasma cells, CD8 + T cells, activated memory CD4 + T cells, naive B cells, and tumor mutation burden. (**L**) Correlation between LY6E and other immune-related genes. Red indicates positive correlation, while blue stands for negative correlation. The darker the color, the stronger the correlation coefficient. *, $p < 0.05$. **, $p < 0.01$. ***, $p < 0.001$.

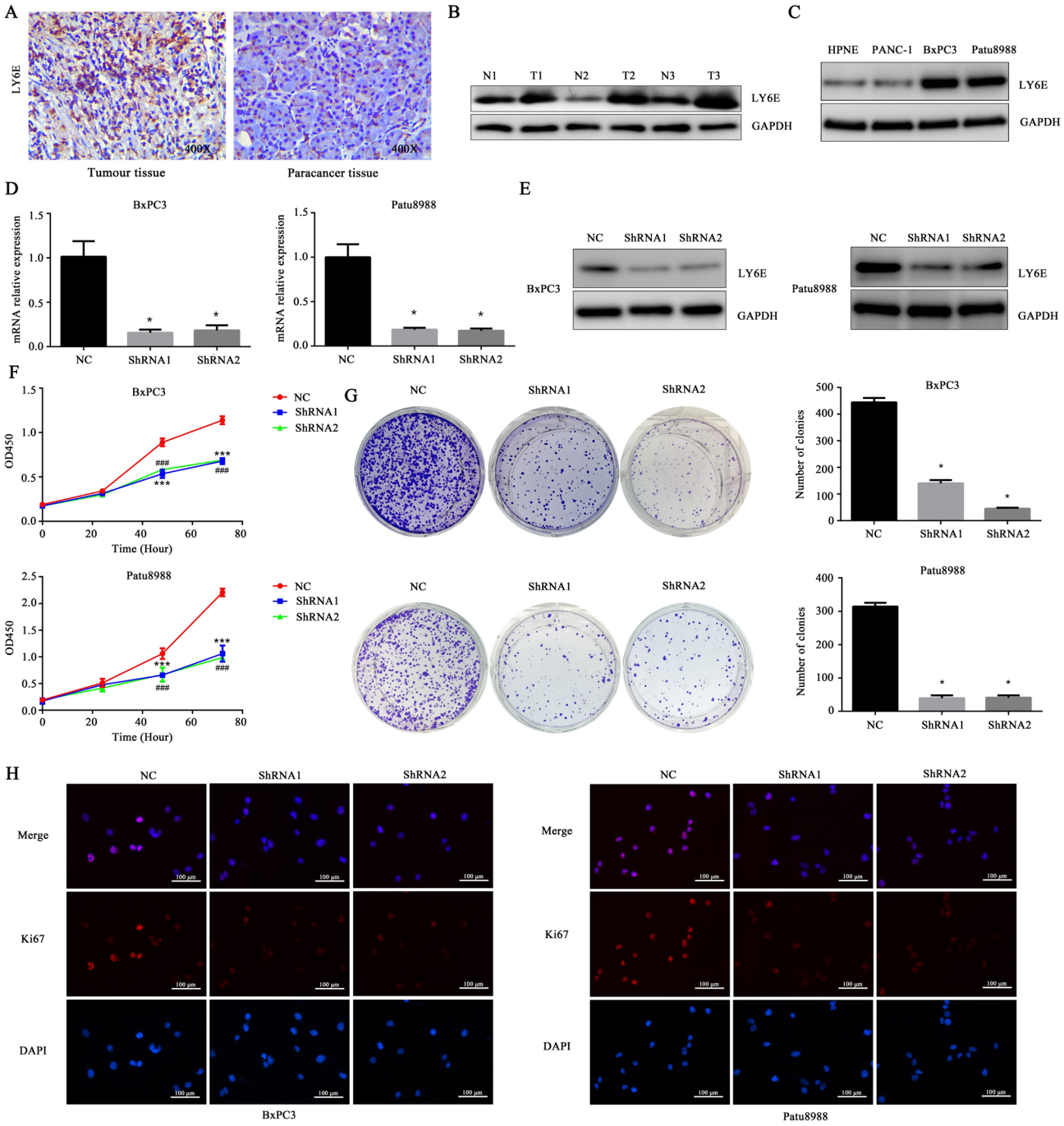

Fig. 4. LY6E is highly expressed in PC and knockdown of LY6E impairs PC cell growth in vitro. (**A**) IHC staining of LY6E expression in the tumor and normal tissues of PC patients. Scale bar = 100 μm. (**B**) Western blotting analysis of LY6E protein expression in tumor tissues and normal tissues of PC patients. GAPDH was used as a control. (**C**) Western blotting analysis of LY6E protein expression in a human pancreatic cell line (HPNE) and PC cell lines (PANC-1, BxPC-3, and Patu8988). GAPDH was used as the control. (**D**) qRT-PCR analysis of LY6E mRNA transcription in BxPC-3 and Patu8988 cells transfected with lenti-shLY6E-1 and lenti-shLY6E-2. GAPDH was used as the control. (**E**) Western blotting analysis of LY6E in BxPC-3 and Patu8988 cells transfected with lenti-shLY6E-1 and lenti-shLY6E-2. GAPDH was used as the control. (**F**) Cell viability at 0, 24, 48 and 72 h were detected after cell was seeded using the CCK-8 assay. OD450 nm absorbance was measured. *** represents the lenti-shLY6E-1 treatment group compared to NC, with $p < 0.001$. ### represents the lenti-shLY6E-2 treatment group compared to NC, with $p < 0.001$. (**G**) Colony formation analysis of BxPC-3 and Patu8988 cells that were transfected with lenti-shLY6E-1 and lenti-shLY6E-2 (14 d after cell seeding). The number of colonies in each well was counted. (**H**) IFC staining of Ki67 in BxPC-3 and Patu8988 cells transfected with lenti-shLY6E-1 and lenti-shLY6E-2.*, $p < 0.05$.

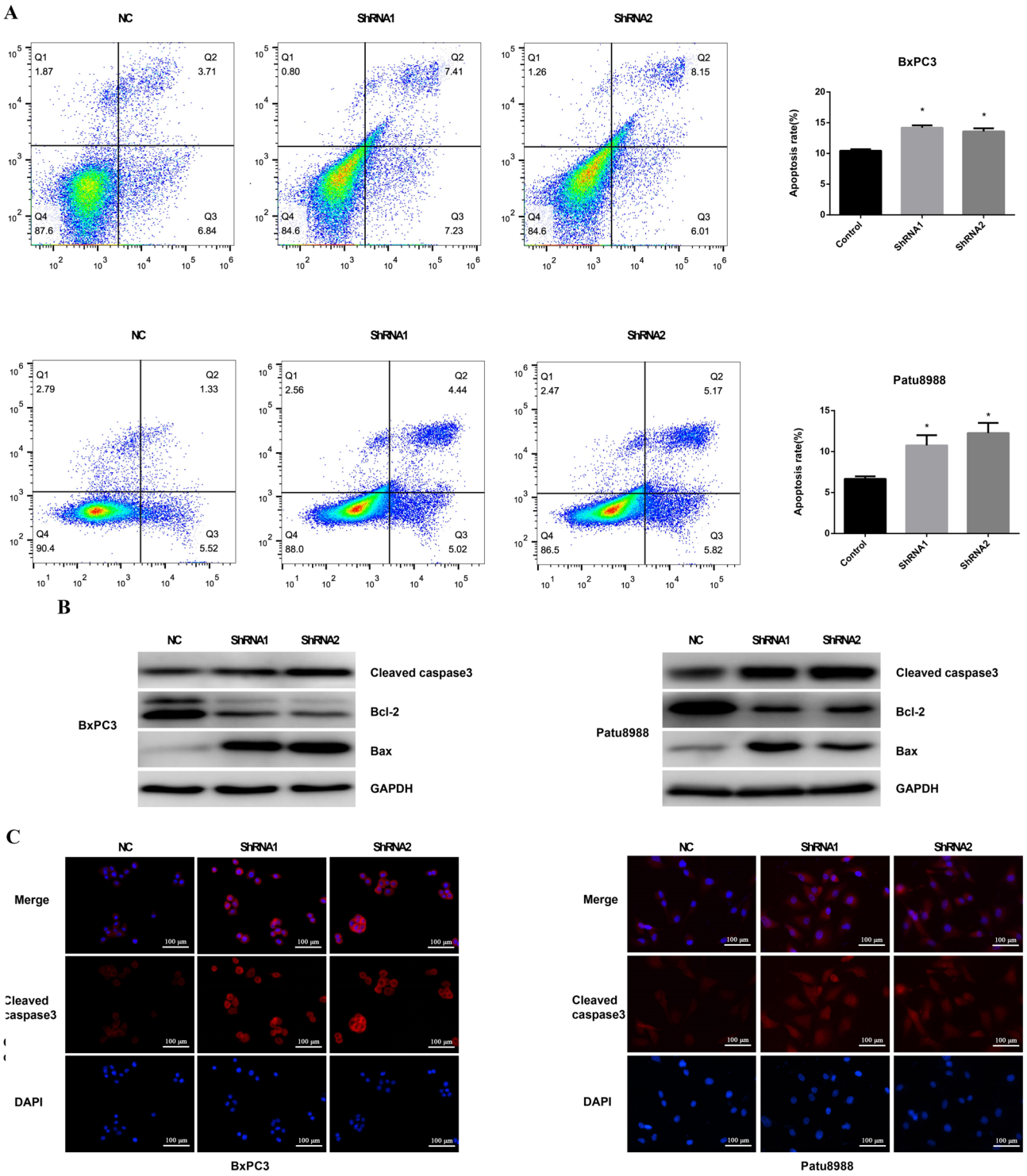

Fig. 5. Knockdown of LY6E promotes apoptosis by regulating cleaved caspase 3, Bcl-2, and Bax protein expression in PC. (**A**) Cell apoptosis was detected in BxPC-3 and Patu8988 cells that were transfected with lenti-shLY6E-1 and lentishLY6E-2. Flow cytometry was used to determine the percentage of cells that were apoptotic. (**B**) Western blotting analysis of cleaved caspase 3, Bcl-2, and Bax protein expression in BxPC-3 and Patu8988 cells that were transfected with lenti-shLY6E-1 and lentishLY6E-2. GAPDH was used as the control. (**C**) IFC staining of cleaved caspase 3 in BxPC-3 and Patu8988 cells transfected with lenti-shLY6E-1 and lenti-shLY6E-2. *, $p < 0.05$.

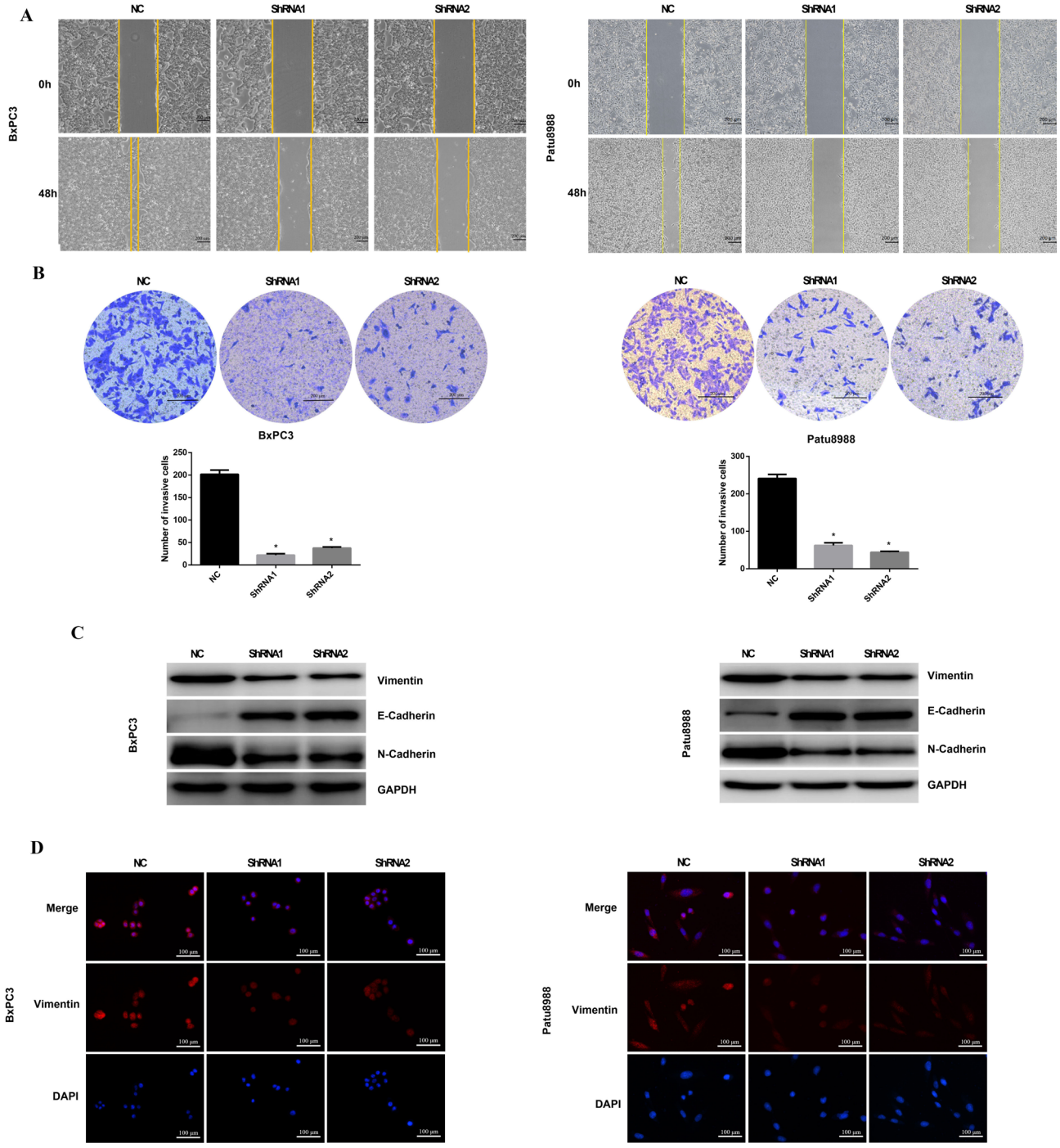

Fig. 6. Knockdown of LY6E suppresses migration and invasion of PC by regulating vimentin, E-Cadherin, and N-Cadherin protein expression. (**A**) Wound healing assay of BxPC-3 and Patu8988 cells that were transfected with lenti-shLY6E-1 and lentishLY6E-2. (**B**) Transwell assay of BxPC-3 and Patu8988 cells that were transfected with lenti-shLY6E-1 and lentishLY6E-2. (**C**) Western blotting analysis of certain migration-related proteins including vimentin, E-Cadherin, and N-Cadherin in BxPC-3 and Patu8988 cells that were transfected with lenti-shLY6E-1 and lentishLY6E-2. GAPDH was used as the control. (**D**) IFC staining of vimentin in BxPC-3 and Patu8988 cells transfected with lenti-shLY6E-1 and lenti-shLY6E-2. *, $p < 0.05$.

in PANC-1 cells (Fig. 7B), suggesting that LY6E promotes cell proliferation. Additionally, LY6E overexpression inhibited apoptosis in PANC-1 cells (Fig. 7C). Transwell assays revealed that LY6E overexpression strengthened the invasive capability of PANC-1 cells (Fig. 7D).

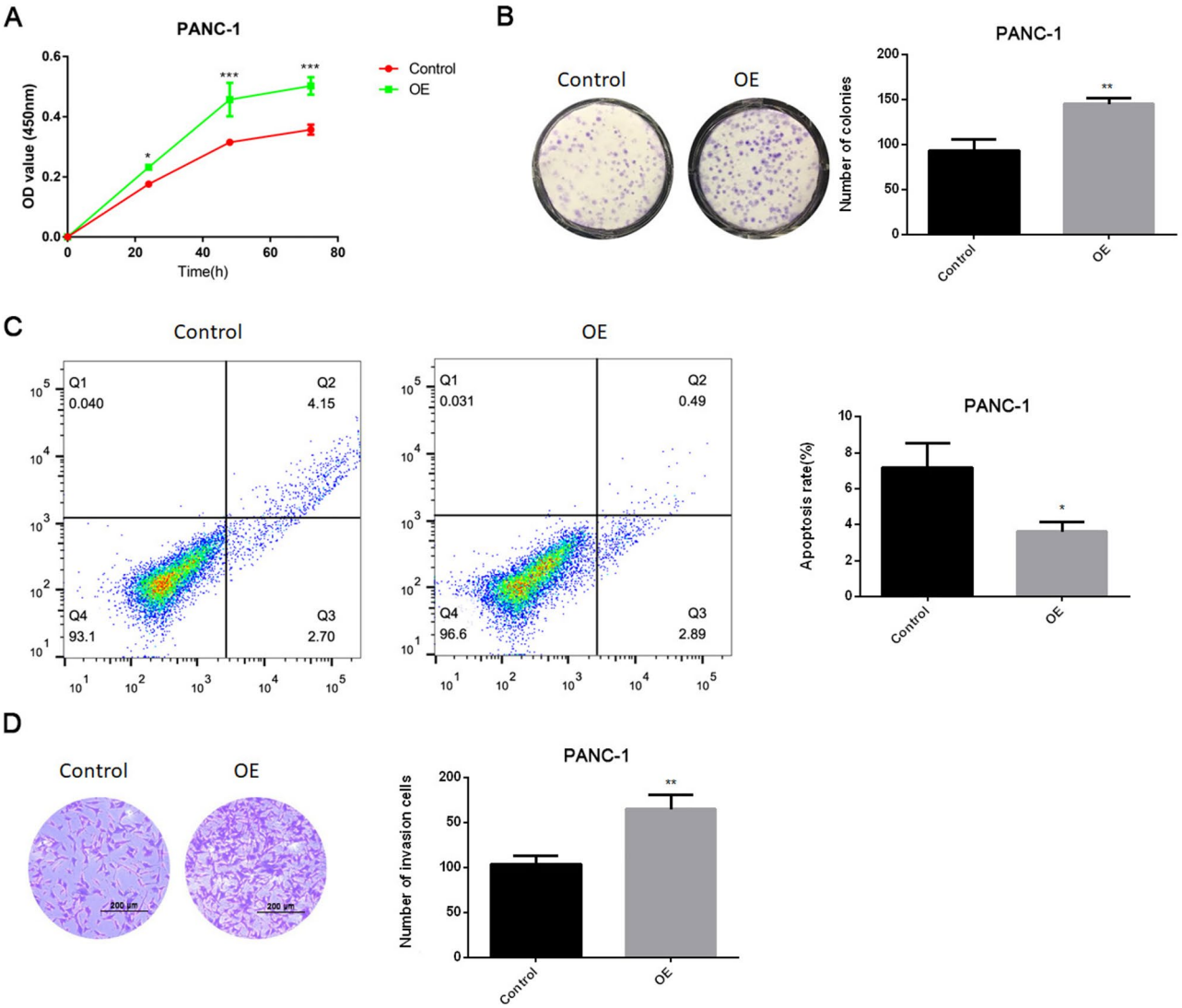

Fig. 7. Overexpression of LY6E suppresses apoptosis, enhances proliferation and migration of PC cells. (**A**) CCK8 assay indicated that overexpression of LY6E augmented PC proliferation. (**B**) Clone formation assay indicated more colonies in LY6E overexpression in PC than in control. **(C)** The effect of LY6E overexpression on PC apoptosis was analyzed by flow cytometry. (**D**) Transwell showed that LY6E increased the number of migrating PC. *, $p < 0.05$. **, $p < 0.01$. ***, $p < 0.001$.

Knockdown of LY6E regulates the Wnt/β-catenin signaling pathway in pancreatic cancer

To deeply explore the underlying molecular mechanism behind the function of LY6E promoting PC development, we identified a putative pathway related with LY6E and validated it in vitro experiment. The heatmap presented the mRNA expression profile between LY6E low-expression and LY6E high-expression PC (Fig. 8A), while the volcano plot showing the up-regulated and down-regulated differential genes between two subgroups (Fig. 8B). Afterward, Gene Ontology (GO) and Kyoto Encyclopedia of Genes and Genomes (KEGG) enrichment analyses were conducted to identify the putative mechanisms of LY6E in PC (Fig. 8C). Based on the KEGG analysis results, the Wnt/β-catenin signaling pathway was confirmed the most related pathway of up-regulated genes (Fig. 8C). Then, the correlation between LY6E and CTNNB1 (the gene encodes β-catenin protein) was analyzed, showing a significant relationship ($P < 0.05$) (Fig. 8D). To verify the regulation of LY6E in Wnt/β-catenin signaling pathway, Western blotting was performed to detect the protein expression of β-catenin, GSK3β, and p-GSK3β, all of which involved in the Wnt/β-catenin signaling pathway (Fig. 8E). Western blotting analysis showed that knockdown of LY6E significantly decreased the β-catenin, while no significant change of GSK3β but reducing the p-GSK3β (Fig. 8E). Immunofluorescence demonstrated that the knockdown of LY6E obviously diminished the expression of β-catenin protein (Fig. 8F).

Knockdown of LY6E impairs pancreatic cancer growth in Vivo

To further evaluate the effect of LY6E in PC, we conduct the in vivo experiment. We collected the Patu8988 cells to establish a xenograft model. Results showed that the knockdown of LY6E effectively inhibited the growth of

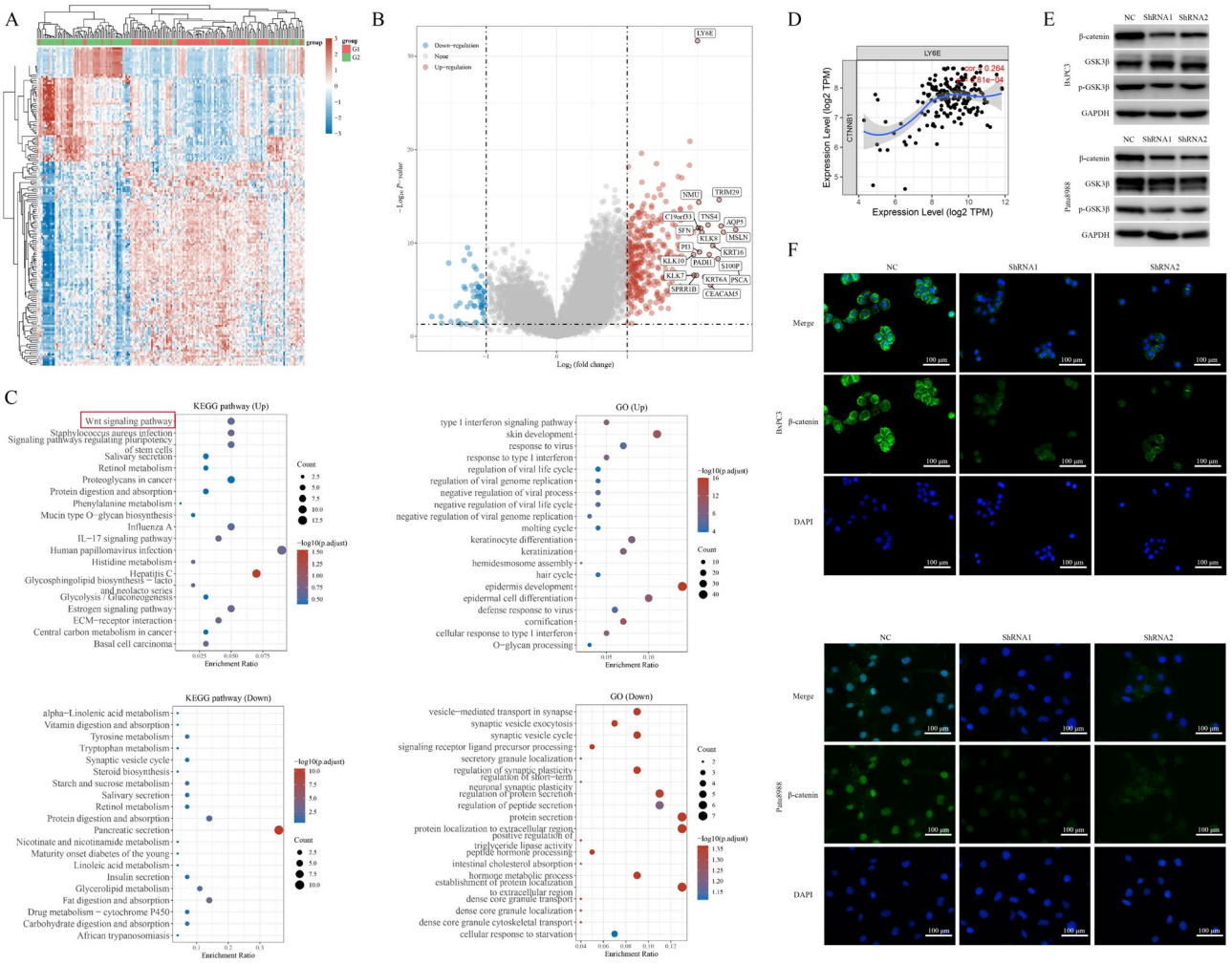

Fig. 8. Knockdown of LY6E down-regulated the Wnt/beta-catenin signaling pathway. (**A**) Gene expression profile of LY6E low-expression and high-expression PC in TCGA-PAAD. G1 and G2 represent groups with high and low expression of LY6E mRNA. Columns and rows denote patients and genes. (**B**) Up-regulated and down-regulated genes in LY6E low-expression and high-expression PC in TCGA-PAAD. Red dots and blue dots indicate upregulated and downregulated genes. The x-axis represents fold change, while the y-axis reflects statistical significance. (**C**) GO/KEGG analysis of up-regulated and down-regulated genes in LY6E low-expression and high-expression PC in TCGA-PAAD. (**D**) Correlation analysis of LY6E expression and CTNNB1 expression. Points represent patients, with the horizontal and vertical axes displaying the expression levels of LY6E and CTNNB1, respectively. (**E**) Western blotting analysis of β-catenin, GSK3β, and p-GSK3β in BxPC-3 and Patu8988 cells that were transfected with lenti-shLY6E-1 and lentishLY6E-2. GAPDH was used as the control. (**F**) IFC staining of β-catenin in BxPC-3 and Patu8988 cells transfected with lenti-shLY6E-1 and lenti-shLY6E-2.

PC (Fig. 9A). Comparing with the control group, tumor weight and tumor volume of the lenti-shLY6E-1 and lenti-shLY6E-2 group was significantly decreased ($P < 0.05$) (Fig. 9B and C). Additionally, Western blotting of migration-related protein in murine PC tissues showed significant increase of E-Cadherin and significant decrease of N-Cadherin and vimentin (Fig. 9D). Immunohistochemistry of murine PC tissues showed the reduction of Ki67, β-catenin, and cleaved caspase 3 protein expression after the knockdown of LY67 (Fig. 9E).

Rescue experiment validating the mechanism of LY6E

To validate the function of LY6E through Wnt/β-catenin signaling pathway, we used the Wnt/β-catenin activator lithium chloride (LiCl) to conduct the rescue experiment. Results showed that the lenti-shLY6E PC cells treated with LiCl recovered the ability of proliferation (Fig. 10A). Moreover, Western blotting analysis confirmed the restoration of migration-related protein including (E-Cadherin, N-Cadherin, and vimentin) and Wnt/β-catenin signaling pathway-related protein (β-catenin, GSK3β, and p-GSK3β) after LiCl treatment to lenti-shLY6E PC cells (Fig. 10B and C).

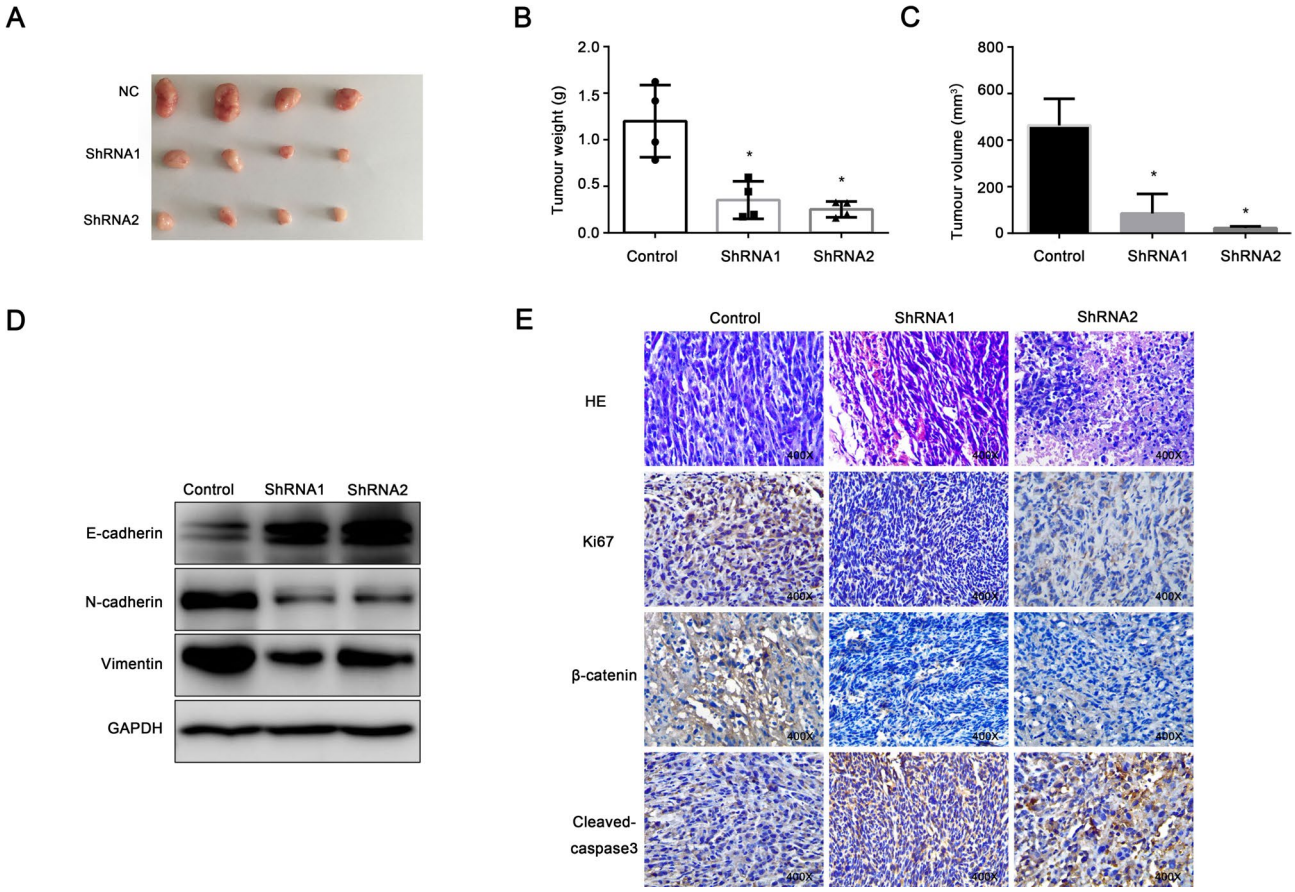

Fig. 9. Knockdown of LY6E inhibits pancreatic tumor growth in vivo. (**A**, **B**, and **C**) Tumor image, end-stage tumor weight, and tumor volume (**D**) Western blotting analysis of Vimentin, E-Cadherin, and N-Cadherin protein expression in tumor tissues. GAPDH was used as the control. (**E**) HE staining and IHC staining of Ki67, β-catenin, and Cleaved caspase 3 in tumor tissues. *, $p < 0.05$.

Discussion

Previous studies have suggested that cancer can result from alterations or abnormal expression of specific cancer-related genes, initiating tumorigenesis or enabling immune evasion by tumor cells[23]. More and more scholars argue that cancer is a genetic disease[24]. Among various cancers, PC stands out with a dismal 5-year overall survival rate of less than 7%[25]. The intricate genetic variations in PC have therefore become a focal point for researchers investigating its progression mechanisms. Identifying novel biomarkers in PC to predict survival and guide targeted therapies is crucial for overcoming this disease.

In recent decades, targeted therapies have been extensively researched, and inhibitors such as programmed death 1 (PD-1) or programmed death ligand 1 (PD-L1) have proven effective in treating various cancers[26,27]. As is known to all, PD-1 expressed by activated T cells, is involved in programmed cell death[28,29]. Tumor-associated PD-L1 was demonstrated to promote T cell apoptosis, thereby preventing tumor cells from being diminished[30]. However, single-agent PD-1/PD-L1 blockade has shown limited efficacy in PC. The unique characteristics of PC contribute to the scarcity of effective treatments[31]. In our study, we confirmed that LY6E is highly expressed in pancreatic cancer (PC) and is closely related to patient clinical characteristics, showing potential as a promising biomarker. Mouse LY6E gene is found expressed in diverse immune cells, including immature T-cells, activated T cells, B cells, and macrophages[32]. Previous evidence and our study results indicated that LY6E might have a potential for PC treatment. Actually, the anti-LY6E antibody has been confirmed an effective measure to suppress development of solid tumors. Tolaney et al. demonstrated that DLYE5953A, an antibody–drug conjugate consisting of an anti-LY6E antibody, had an acceptable safety and a considerable antitumor activity at 2.4 mg/kg for HER2-negative metastatic breast cancer and non–small cell lung cancer[33]. Additionally, Asundi et al. confirmed that an antibody–drug conjugate directed against LY6E showed strong tumor killing in a number of cancers[12]. The emergence of inhibitors targeting LY6E presents a new opportunity. RG-7841specifically binds to and inhibits LY6E activity, potentially serving as a direct therapeutic strategy for PC. However, its effectiveness and safety require further evaluation. So far, natural drugs targeting LY6E have not yet been identified. Importantly, from our study, we identified that LY6E expression was closely related with immune cell infiltration, such as dendric cells, macrophages, or NK cells, all of which played vital roles in tumor progression. Besides, the correlation between LY6E and immune-related genes was identified in our study. From the immunity analysis of LY6E, we speculated that LY6E expression might have the potential to predict immunotherapy response. Based on other

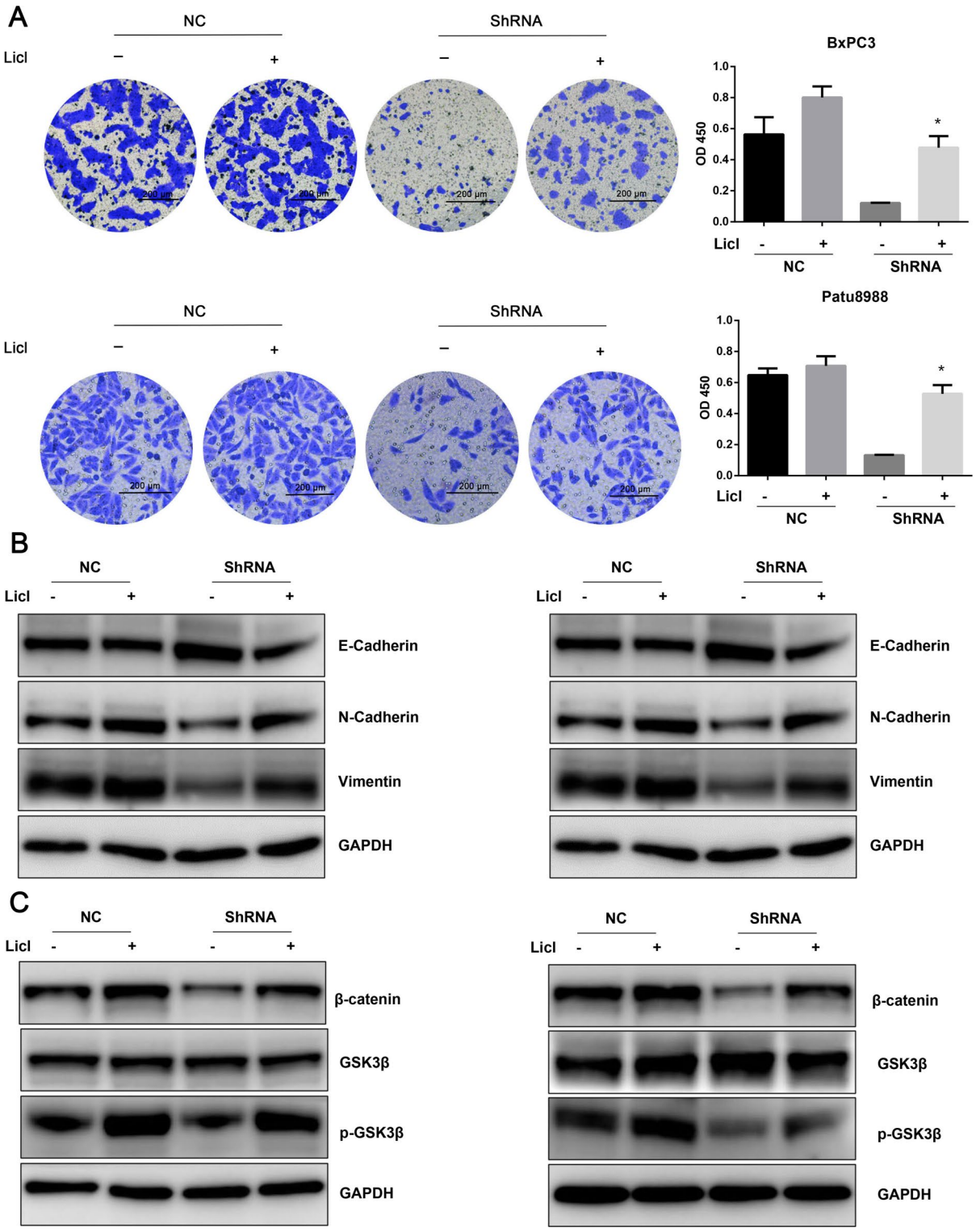

Fig. 10. The rescue experiment verifies that LY6E promotes PC progression through Wnt/beta-catenin signaling pathway. (**A**) Transwell assay confirmed the restoration of invasion of BxPC-3 and Patu8988 cells transfected with lenti-shLY6E after being treated by LiCl. (**B** and **C**) Western blotting analysis of Vimentin, E-Cadherin, N-Cadherin, β-catenin, GSK3β, and p-GSK3β protein expression in BxPC-3 and Patu8988 cells transfected with lenti-shLY6E after treated by LiCl. GAPDH was used as the control. *, $p < 0.05$.

studies and our analysis, we can safely conclude that the immune-related gene LY6E had the potential to guide therapy or even be the target to treat PC.

In past publications, increasing expression of LY6E was related with poor prognosis in various cancers, including renal papillary cell carcinoma, bladder cancer, gastric cancer, and hepatocellular carcinoma[34]. According to our analysis, the prognostic capacity of LY6E in PC has been confirmed, and the Cox regression analysis even revealed that LY6E can be an independent prognostic factor for PC. Despite other proofs of high-expression mRNA of LY6E in PC and might stimulate PC stem cells proliferating[16], detailed mechanisms of LY6E in PC are unclear. Our in vivo and in vitro experiments demonstrated that LY6E can promote PC cell proliferation and tumor growth in mice. Furthermore, migration-related proteins, vimentin, E-Cadherin, and N-Cadherin all have been found regulated by LY6E expression in our study, leading to the migration of PC cells. Additionally, our research confirmed knockdown of LY6E increasing the apoptosis of PC mediated with cleaved caspase 3, Bcl-2, and Bax, while overexpression of LY6E reduced the proportion of apoptotic cells. The functions of enhancing proliferation, inhibiting apoptosis, and facilitating migration might account for the poor outcome caused by LY6E's high expression in PC.

From our functional enrichment analysis, we identified several putative pathways that might mediate the function of LY6E in PC, like Wnt/β-catenin signaling pathway, IL-17 signaling pathway, and ECM-receptor interaction pathway. We confirmed the function of high-expression LY6E via up-regulating Wnt/β-catenin signaling pathway to promote migration of PC. Wnt/β-catenin signaling pathway has been proven to play important roles in PC development with abundant evidence[35,36]. Our study found and verified the relationship between LY6E and Wnt/β-catenin signaling pathway. Undoubtedly, our study uncovered the veil of LY6E in PC. Additionally, previous research confirmed that LY6E signaling to TGF-β can promote breast cancer progression[16], while PTEN and PI3K/Akt signaling pathways are related with LY6E-mediated augment of HIF-1α[16]. Wnt/β-catenin signaling pathway has been proven related with TGF-β, PI3K/Akt, and HIF-1 signaling pathways[37,38]. We speculated that there might been some connection between LY6E, Wnt/β-catenin signaling pathway, and other signaling pathways.

There are still some limitations that need to be considered. First, we do not have enough clinical patient samples to verify the prognostic ability of LY6E expression in the real world. However, we are collecting clinical PC samples, and carrying on the follow-up for the patients. In addition, there are diverse downstream effectors of Wnt/β-catenin signaling pathway have been functioning in tumor progression and complex interaction between Wnt/β-catenin signaling pathway and other pathways. To further explore the mechanism of LY6E in PC, we are planning to conduct deeper research for LY6E.

Conclusions

The study strongly suggested that LY6E is highly expressed in the PC and demonstrated an independent prognostic factor. Additionally, LY6E was confirmed related with immunity. Besides, LY6E promoted PC development, apoptosis and migration by up-regulation of Wnt/β-catenin signaling pathway.

Materials and methods

Online data extraction and process

The GEPIA2 (Gene Expression Profiling Interactive Analysis, version 2) tool (http://gepia2.cancer-pku.cn/#analysis) was used to conduct the LY6E expression in PC tissues and normal tissues. The expression of LY6E was analyzed in GSE16515, GSE32676, GSE15471, and GSE55463 datasets (http://www.ncbi.nlm.nih.gov/geo/)[39–42]. The "limma" R package was used to evaluate the LY6E expression in different subgroups and the correlation between LY6E expression and clinical characteristics was visualized with a Sanky plot[43]. Furthermore, Kaplan–Meier (K–M) analysis for TCGA-PAAD project was conducted to confirm the LY6E a prognostic gene in PC[44]. The AUC (area under the receiver operating characteristic (ROC) curve) values of the TCGA-PAAD were used to determine LY6E's prognostic value[45]. We conducted univariate and multivariate Cox regression analyses to identify independent prognostic factors for PC. The "rms" R package was used to construct a nomogram with the independent prognostic factors, while the calibration curve was used to determine the predictive probability of the nomogram [46]. The correlation between LY6E and immune cell was assessed by Pearson's correlation coefficient and the immune cell infiltration was evaluated by CIBERSORT algorithm[47,48]. The correlation between LY6E and diverse immune-related genes was presented in a heatmap.

Cell culture and transfection

The PC cell lines (BxPC-3, PANC-1, and Patu8988) and human pancreatic ductal epithelial cell line (HPNE) were obtained from the Cell Bank of the Shanghai Institute of Biochemistry and Cell Biology (Shanghai, China). The cell lines were cultivated in Dulbecco's modified Eagle's medium and added with 10% fetal bovine serum (FBS), 100 μg/ml streptomycin, and 100 U/ml penicillin (Gibco). LY6E-targeting short hairpin RNA (sh-LY6E) and non-specific control shRNA (sh-NC) were obtained from Sigma, along with the overexpression plasmid (OE-LY6E). The shRNA sequences used were as follows: GAAGAGCAATCTGTACTGCCT and CATTGGGAA TCTCGTGACATT. The PC cell lines were transfected with lentivirus-sh-LY6E, and the stably transfected PC cell lines were identified using puromycin (2 mg/mL)[49].

Immunohistochemistry

Immunohistochemical staining was conducted as described previously[49], with the anti-human LY6E, Ki67, β-catenin, and cleaved caspase 3 rabbit Ab (1:100) obtained from the Abcam; PBS was used as a negative control. Paraffin sections were prepared from patient tumor tissues and xenograft tumor tissues. The clinical samples were collected from the First Affiliated Hospital of Wenzhou Medical University and the study was supported by

the Ethics Committee of the First Clinical Medical College of Wenzhou Medical University (Approval Number: 201911).

Western blotting

Western blotting analysis was conducted as previously described[49]. The following primary Abs were used: LY6E rabbit polyclonal Ab (ab201098, 1:1000, Abcam), β-catenin rabbit monoclonal Ab (ab32572, 1:1000, Abcam), GSK3β rabbit monoclonal Ab (ab32391, 1:1000, Abcam), p-GSK3β rabbit monoclonal Ab (ab75814, 1:1000, Abcam), E-cadherin rabbit monoclonal Ab (ab40772, 1:1000, Abcam), N-cadherin rabbit monoclonal Ab (ab76011, 1:1000, Abcam), Vimentin rabbit monoclonal Ab (ab92547, 1:1000, Abcam), Bcl-2 rabbit monoclonal Ab (ab32124, 1:1000, Abcam), Bax rabbit monoclonal Ab (ab32503, 1:1000, Abcam), Cleaved caspase3 rabbit monoclonal Ab (ab32042, 1:1000, Abcam) and GAPDH mouse monoclonal Ab (ab8245, 1:1000, Abcam).

Quantitative reverse transcriptase-PCR

BxPC-3, and Patu8988 cells were washed with PBS and then homogenized in TRIzol reagent (Invitrogen). Total RNA was extracted and reverse transcribed into cDNA template and then SYBR Green Real-Time PCR Master Mix Plus (Toyobo) was used for QRT-PCR. β-ACTIN was used as an endogenous reference gene[32]. The primer sequences for amplification were as follows: forward 5′- TGCGGAAGGGGACGAGGGTTC-3′ and reverse 5′- CGTACACAGCCAGGCACACATC-3′ for LY6E, and forward 5′-TGACGTGGACATCCGCAAAG-3′ and reverse 5′-CTGGAAGGTGGACAGCGAGG-3′ for β-ACTIN.

Cell viability assay and colony formation assay

Cell viability was evaluated by Cell Counting Kit-8 (CCK-8; Dojindo, Shanghai, China) following the protocol of manufacturer. Transfected PC cells were plated at a density of 2 × 103 cells per well in 96-well plates. Sequentially, we measured the absorbance at 450 nm at different time points (Thermo Fisher Scientific, Waltham, MA, USA)[49].

Transfected pancreatic cancer cells were plated at a density of 1000 cells per well in six-well plates and allowed to grow for 14 days to form colonies. Following incubation, the cells were stained with crystal violet, and the resulting colonies were visualized and counted to assess their growth and proliferation capabilities[49].

Wound healing assay and transwell assay

Cell migration and invasion abilities were evaluated using wound healing and transwell assays. Transfected PC cells were seeded at 5×10^5 cells per well, and cultivated until reaching 100% confluence. The cells were scratched using a 10 μl pipette tip (Sigma) and washed using PBS for three times. Sequentially, the cells were cultured for an additional 48 h. Finally, we used microscopy to identify the extent of wound closure[49].

Transfected PC cells were seeded at 4×10^5 cells per upper transwell chamber, cultivated with 100 mL of reconstituted Matrigel-coated membrane for 36–48 h. Thereafter, the cell number of invading PC was counted[49].

Flow cytometry assay

The apoptosis of PC cells was detected using the Annexin V-FITC/PI kit (Keygentec) according to the protocol of manufacturer. Flow cytometry analysis was carried out using a BD LSRII Flow Cytometer (Becton Dickson). BD FACSDiva was used to analyze the data[49].

Animal experiment

Patu8988 cells were injected subcutaneously into the flanks of 6–8 weeks-old female nude mice. All mice were cultivated with free food and water in a specific pathogen-free environment. Tumor volume was calculated as follows: Volume = (length × width^2)/2[49]. The animal study was approved by the Institutional Animal Care and Use Committee of Wenzhou Medical University, China. Animal experiments were performed according to all regulatory and institutional guidelines for animal welfare (National Institutes of Health Publications, NIH Publications No. 80–23). Ethical approval (WYYY-AEC-2021–290) for this study was obtained from the Ethics Committee of the First Affiliated Hospital of Wenzhou Medical University. Our research complies with the ARRIVE guidelines (https://arriveguidelines.org).

Statistical analysis

All experimental data are presented as mean ± SD and are representative of at least 3 independent experiments. Statistical analyses were conducted using R- × 64–4.1.1 and Graphpad Prism tools. Differences with $P < 0.05$ were considered statistically significant.

Data availability

All data used to support the findings of this study are available from the corresponding author upon request.

Received: 10 June 2024; Accepted: 21 August 2024
Published online: 30 August 2024

References

1. Wang, Y. *et al.* Inhibition of autophagy induced by tetrandrine promotes the accumulation of reactive oxygen species and sensitizes efficacy of tetrandrine in pancreatic cancer. *Cancer Cell Int.* **24**, 241. https://doi.org/10.1186/s12935-024-03410-5 (2024).
2. The global, regional, and national burden of pancreatic cancer and its attributable risk factors in 195 countries and territories, 1990–2017: A systematic analysis for the Global Burden of Disease Study 2017. Lancet Gastroenterol. Hepatol. **4**:934–947 (2019). https://doi.org/10.1016/s2468-1253(19)30347-4

3. Pulvirenti, A. *et al.* Integrating metabolic profiling of pancreatic juice with transcriptomic analysis of pancreatic cancer tissue identifies distinct clinical subgroups. *Front Oncol.* **14**, 1405612. https://doi.org/10.3389/fonc.2024.1405612 (2024).
4. Zheng, B. *et al.* Development and external validation of a prognostic nomogram to predict survival in patients aged ≥ 60 years with pancreatic ductal adenocarcinoma. *Transl. Cancer Res.* **13**, 2751–2766. https://doi.org/10.21037/tcr-24-5 (2024).
5. Yang, Y. *et al.* LINC01133 promotes pancreatic ductal adenocarcinoma epithelial-mesenchymal transition mediated by SPP1 through binding to Arp3. *Cell Death Dis.* **15**, 492. https://doi.org/10.1038/s41419-024-06876-3 (2024).
6. Anandhan, S. *et al.* TSG-6+ cancer-associated fibroblasts modulate myeloid cell responses and impair anti-tumor response to immune checkpoint therapy in pancreatic cancer. *Nat. Commun.* **15**, 5291. https://doi.org/10.1038/s41467-024-49189-x (2024).
7. Saluja, A. *et al.* Pancreatitis and pancreatic cancer. *Gastroenterology* **156**, 1937–1940. https://doi.org/10.1053/j.gastro.2019.03.050 (2019).
8. Offit, K. *et al.* Cascading after peridiagnostic cancer genetic testing: An alternative to population-based screening. *J. Clin. Oncol.* **38**, 1398–1408. https://doi.org/10.1200/jco.19.02010 (2020).
9. Childers, K. K. *et al.* National distribution of cancer genetic testing in the United States: Evidence for a gender disparity in hereditary breast and ovarian cancer. *JAMA Oncol.* **4**, 876–879. https://doi.org/10.1001/jamaoncol.2018.0340 (2018).
10. Rustgi, A. K. Familial pancreatic cancer: Genetic advances. *Genes Dev.* **28**, 1–7. https://doi.org/10.1101/gad.228452.113 (2014).
11. Gumley, T. P. *et al.* Tissue expression, structure and function of the murine Ly-6 family of molecules. *Immunol. Cell Biol.* **73**, 277–296. https://doi.org/10.1038/icb.1995.45 (1995).
12. Asundi, J. *et al.* An antibody-drug conjugate directed against lymphocyte Antigen 6 complex, locus E (LY6E) provides robust tumor killing in a wide range of solid tumor malignancies. *Clin. Cancer Res.* **21**, 3252–3262. https://doi.org/10.1158/1078-0432.Ccr-15-0156 (2015).
13. Benguigui, M. *et al.* Interferon-stimulated neutrophils as a predictor of immunotherapy response. *Cancer Cell* **42**, 253-265.e212. https://doi.org/10.1016/j.ccell.2023.12.005 (2024).
14. Tokhanbigli, S. *et al.* Dendritic cell-based therapy using LY6E peptide with a putative role against colorectal cancer. *Immunotargets Ther.* **9**, 95–104. https://doi.org/10.2147/itt.S245913 (2020).
15. Yeom, C. J. *et al.* LY6E: A conductor of malignant tumor growth through modulation of the PTEN/PI3K/Akt/HIF-1 axis. *Oncotarget* **7**, 65837–65848. https://doi.org/10.18632/oncotarget.11670 (2016).
16. AlHossiny, M. *et al.* Ly6E/K signaling to TGFβ promotes breast cancer progression, immune escape, and drug resistance. *Cancer Res.* **76**, 3376–3386. https://doi.org/10.1158/0008-5472.Can-15-2654 (2016).
17. Yang, M. *et al.* The application of nanoparticles in cancer immunotherapy: Targeting tumor microenvironment. *Bioact. Mater* **6**, 1973–1987. https://doi.org/10.1016/j.bioactmat.2020.12.010 (2021).
18. DeBerardinis, R. J. Tumor microenvironment, metabolism, and immunotherapy. *N. Engl. J. Med.* **382**, 869–871. https://doi.org/10.1056/NEJMcibr1914890 (2020).
19. Singleton, D. C. *et al.* Therapeutic targeting of the hypoxic tumour microenvironment. *Nat. Rev. Clin. Oncol.* **18**, 751–772. https://doi.org/10.1038/s41571-021-00539-4 (2021).
20. Connor, A. A. *et al.* Pancreatic cancer evolution and heterogeneity: Integrating omics and clinical data. *Nat. Rev. Cancer* **22**, 131–142. https://doi.org/10.1038/s41568-021-00418-1 (2022).
21. Ho, W. J. *et al.* The tumour microenvironment in pancreatic cancer—clinical challenges and opportunities. *Nat. Rev. Clin. Oncol.* **17**, 527–540. https://doi.org/10.1038/s41571-020-0363-5 (2020).
22. Mar, K. B. *et al.* LY6E mediates an evolutionarily conserved enhancement of virus infection by targeting a late entry step. *Nat. Commun.* **9**, 3603. https://doi.org/10.1038/s41467-018-06000-y (2018).
23. Martincorena, I. *et al.* Somatic mutation in cancer and normal cells. *Science* **349**, 1483–1489. https://doi.org/10.1126/science.aab4082 (2015).
24. Tomasetti, C. *et al.* Cancer etiology. Variation in cancer risk among tissues can be explained by the number of stem cell divisions. *Science* **347**, 78–81. https://doi.org/10.1126/science.1260825 (2015).
25. Kamisawa, T. *et al.* Pancreatic cancer. *Lancet* **388**, 73–85. https://doi.org/10.1016/s0140-6736(16)00141-0 (2016).
26. Feng, Y. Y. *et al.* Synthetic lethal CRISPR screen identifies a cancer cell-intrinsic role of PD-L1 in regulation of vulnerability to ferroptosis. *Cell Rep.* **43**, 114477. https://doi.org/10.1016/j.celrep.2024.114477 (2024).
27. Wang, L. *et al.* A novel bispecific peptide targeting PD-1 and PD-L1 with combined antitumor activity of T-cells derived from the patients with TSCC. *Int. Immunopharmacol.* **138**, 112582. https://doi.org/10.1016/j.intimp.2024.112582 (2024).
28. Law, C. *et al.* Interferon subverts an AHR-JUN axis to promote CXCL13(+) T cells in lupus. *Nature*. https://doi.org/10.1038/s41586-024-07627-2 (2024).
29. Okita, R. *et al.* Characterizing soluble immune checkpoint molecules and TGF-β(1,2,3) in pleural effusion of malignant pleural mesothelioma. *Sci. Rep.* **14**, 15947. https://doi.org/10.1038/s41598-024-66189-5 (2024).
30. Gu, H. *et al.* Myeloma induce Fapα+ macrophage to remodel immune microenvironment which lead to anti-PD-1 dilemma. *Blood* **136**, 22–22. https://doi.org/10.1182/blood-2020-139535 (2020).
31. Feng, M. *et al.* PD-1/PD-L1 and immunotherapy for pancreatic cancer. *Cancer Lett.* **407**, 57–65. https://doi.org/10.1016/j.canlet.2017.08.006 (2017).
32. Lee, P. Y. *et al.* Ly6 family proteins in neutrophil biology. *J. Leukoc. Biol.* **94**, 585–594. https://doi.org/10.1189/jlb.0113014 (2013).
33. Tolaney, S. M. *et al.* A phase I study of DLYE5953A, an Anti-LY6E antibody covalently linked to monomethyl Auristatin E, in patients with refractory solid tumors. *Clin. Cancer Res.* **26**, 5588–5597. https://doi.org/10.1158/1078-0432.Ccr-20-1067 (2020).
34. Luo, L. *et al.* Distinct lymphocyte antigens 6 (Ly6) family members Ly6D, Ly6E, Ly6K and Ly6H drive tumorigenesis and clinical outcome. *Oncotarget* **7**, 11165–11193. https://doi.org/10.18632/oncotarget.7163 (2016).
35. Yu, M. *et al.* RNA sequencing of pancreatic circulating tumour cells implicates WNT signalling in metastasis. *Nature* **487**, 510–513. https://doi.org/10.1038/nature11217 (2012).
36. Zhou, C. *et al.* LncRNA PVT1 promotes gemcitabine resistance of pancreatic cancer via activating Wnt/β-catenin and autophagy pathway through modulating the miR-619-5p/Pygo2 and miR-619-5p/ATG14 axes. *Mol. Cancer* **19**, 118. https://doi.org/10.1186/s12943-020-01237-y (2020).
37. Tenbaum, S. P. *et al.* β-catenin confers resistance to PI3K and AKT inhibitors and subverts FOXO3a to promote metastasis in colon cancer. *Nat. Med.* **18**, 892–901. https://doi.org/10.1038/nm.2772 (2012).
38. Liu, X. *et al.* HIF-1-regulated expression of calreticulin promotes breast tumorigenesis and progression through Wnt/β-catenin pathway activation. *Proc. Natl. Acad. Sci. U. S. A.*. https://doi.org/10.1073/pnas.2109144118 (2021).
39. Li, L. *et al.* Genetic variations associated with gemcitabine treatment outcome in pancreatic cancer. *Pharmacogenet. Genom.* **26**, 527–537. https://doi.org/10.1097/fpc.0000000000000241 (2016).
40. Donahue, T. R. *et al.* Integrative survival-based molecular profiling of human pancreatic cancer. *Clin. Cancer Res.* **18**, 1352–1363. https://doi.org/10.1158/1078-0432.Ccr-11-1539 (2012).
41. Badea, L. *et al.* Combined gene expression analysis of whole-tissue and microdissected pancreatic ductal adenocarcinoma identifies genes specifically overexpressed in tumor epithelia. *Hepatogastroenterology* **55**, 2016–2027 (2008).
42. Sun, T. *et al.* Identification of a microRNA regulator for axon guidance in the olfactory bulb of adult mice. *Gene* **547**, 319–328. https://doi.org/10.1016/j.gene.2014.06.063 (2014).
43. Ritchie, M. E. *et al.* Limma powers differential expression analyses for RNA-sequencing and microarray studies. *Nucleic Acids Res.* **43**, e47. https://doi.org/10.1093/nar/gkv007 (2015).

44. Rich, J. T. *et al.* A practical guide to understanding Kaplan–Meier curves. *Otolaryngol. Head Neck Surg.* **143**, 331–336. https://doi.org/10.1016/j.otohns.2010.05.007 (2010).
45. Metz, C. E. Basic principles of ROC analysis. *Semin. Nucl. Med.* **8**, 283–298. https://doi.org/10.1016/s0001-2998(78)80014-2 (1978).
46. Iasonos, A. *et al.* How to build and interpret a nomogram for cancer prognosis. *J. Clin. Oncol.* **26**, 1364–1370. https://doi.org/10.1200/jco.2007.12.9791 (2008).
47. Schober, P. *et al.* Correlation coefficients: Appropriate use and interpretation. *Anesth. Anal.* **126**, 1763–1768. https://doi.org/10.1213/ane.0000000000002864 (2018).
48. Newman, A. M. *et al.* Robust enumeration of cell subsets from tissue expression profiles. *Nat. Methods* **12**, 453–457. https://doi.org/10.1038/nmeth.3337 (2015).
49. Guo, Y. *et al.* The anthelmintic drug niclosamide induces GSK-β-mediated β-catenin degradation to potentiate gemcitabine activity, reduce immune evasion ability and suppress pancreatic cancer progression. *Cell Death Dis.* **13**, 112. https://doi.org/10.1038/s41419-022-04573-7 (2022).

Author contributions

K.C., J.Z. and X.Y. Wrote original draft Writing and performed data analysis. Y.G. performed the experimental validation. Y.X. designed the study and conducted the data analysis.

Funding

This work is supported by the fund Wenzhou Basic Public Welfare Research Project. (Grant ID: Y2023222).

Competing interests

The authors declare no competing interests.

Additional information

Supplementary Information The online version contains supplementary material available at https://doi.org/10.1038/s41598-024-70764-1.

Correspondence and requests for materials should be addressed to Y.X.

Reprints and permissions information is available at www.nature.com/reprints.

Publisher's note Springer Nature remains neutral with regard to jurisdictional claims in published maps and institutional affiliations.